Load Sculptor: Robust Dynamic Load Modeling and Uncertainty Quantification

DOE Dynamic Load Modeling Workshop

Nan Duan, LLNL

Mar. 24, 2022

LLNL-PRES-XXXXXX

This work was performed under the auspices of the U.S. Department of Energy by Lawrence Livermore National Laboratory under contract DE-AC52-07NA27344. Lawrence Livermore National Security, LLC

Lawrence Livermore National Laboratory

Project Overview

- *Sponsor:*

Ali Ghassemian, DOE Office of Electricity, Advanced Grid Modeling Program

- *Academic Collaborator:*

Junbo Zhao, University of Connecticut

- *Industrial Advisors:*

Song Wang, PacifiCorp

Xiaodong Liu, Eversource Energy

Project Goals

- Develop **computationally cheap surrogate dynamic load models** for dynamic simulation and security assessment without sacrificing the accuracy requirement;
- Derive robust load model parameter sets that are able to capture a wide range of operating conditions;
- **Quantifying the influences of parameter uncertainties** on the simulation results as well as other time-domain simulation-based applications, including transient stability analysis.

Research Overview

- **Bus level**:
  dynamic load models used at a specific bus, IM+ZIP, CMPLDWG, etc.

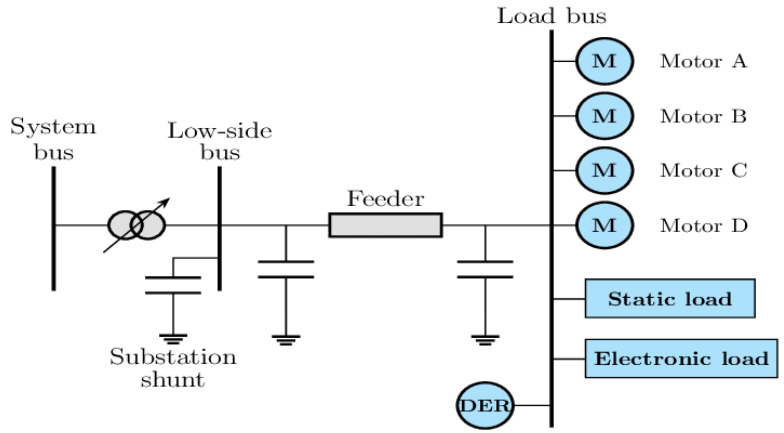

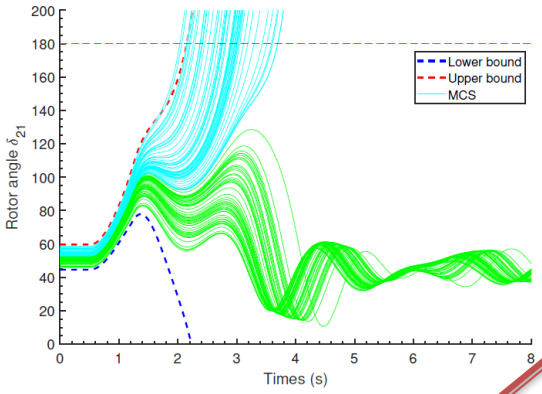

- **System level**:
  Different dynamic load models at different locations

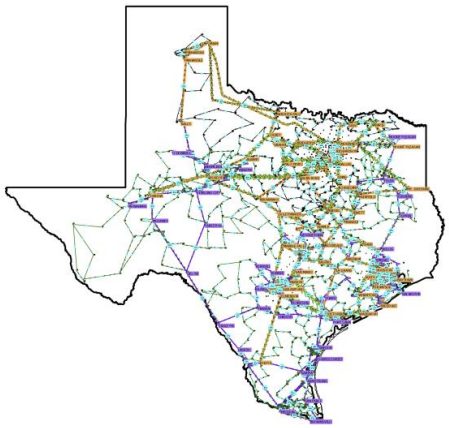

- **Uncertainty sources**:
  Inaccurate dynamic load parameters, varying load compositions, etc.

Research Overview

Bus Level

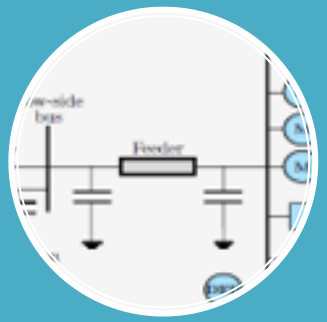

- Machine Learning (ML) based surrogate model;
- Parameter identification and uncertainty quantification (UQ)

System Level

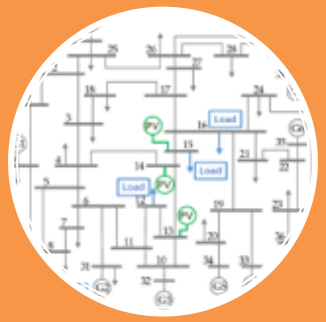

- Reduced order modeling (ROM);
- Sensitivity analysis (SA)
- Frequency variation estimation of load buses with IBRs

Fast and accurate dynamic load simulation for uncertainty quantification of dynamic security analysis (DSA)

Table of Contents

- Stochastic Power System Dynamic Security Assessment Considering Uncertainties from Dynamic Loads and PVs (**Best Conference Paper Award**)
- WECC Composite Load Model Parameter Identification Using Deep Learning Approach
- System-level Reduced Order Modeling of Dynamic Loads

Stochastic Dynamic Security Assessment-Problem Formulation

- Power system stochastic dynamic model with uncertainty is expressed as

$$\begin{cases} \dot{\boldsymbol{x}} = \boldsymbol{f}(\boldsymbol{x}, \boldsymbol{y}, \boldsymbol{u}, \boldsymbol{\xi}) \\ \boldsymbol{0} = \boldsymbol{g}(\boldsymbol{x}, \boldsymbol{y}, \boldsymbol{\xi}) \end{cases}$$

$\boldsymbol{x}$: dynamic state vector; $\boldsymbol{y}$: algebraic state vector; $\boldsymbol{u}$: system input; $\boldsymbol{\xi}$: uncertainty input vector that includes uncertain dynamic loads, and various types of IBRs.

- The relationship between uncertainties and dynamic state vector

$$\boldsymbol{x}(t) = \mathcal{M}(\boldsymbol{\xi}, t)$$

$\boldsymbol{\xi}$: loads and IBRs; $\boldsymbol{x}$**:** generator and IBR dynamic states.

➢ **Objective**: develop computationally efficient approaches for stochastic dynamic security assessment with uncertainties.

Proposed Method

- **Key idea**: develop the **polynomial chaos expansion (PCE) based reduced order dynamic model** with high computationally efficiency without loss of accuracy. PCE coefficients naturally allow us for uncertainty quantification of dynamic simulation results.

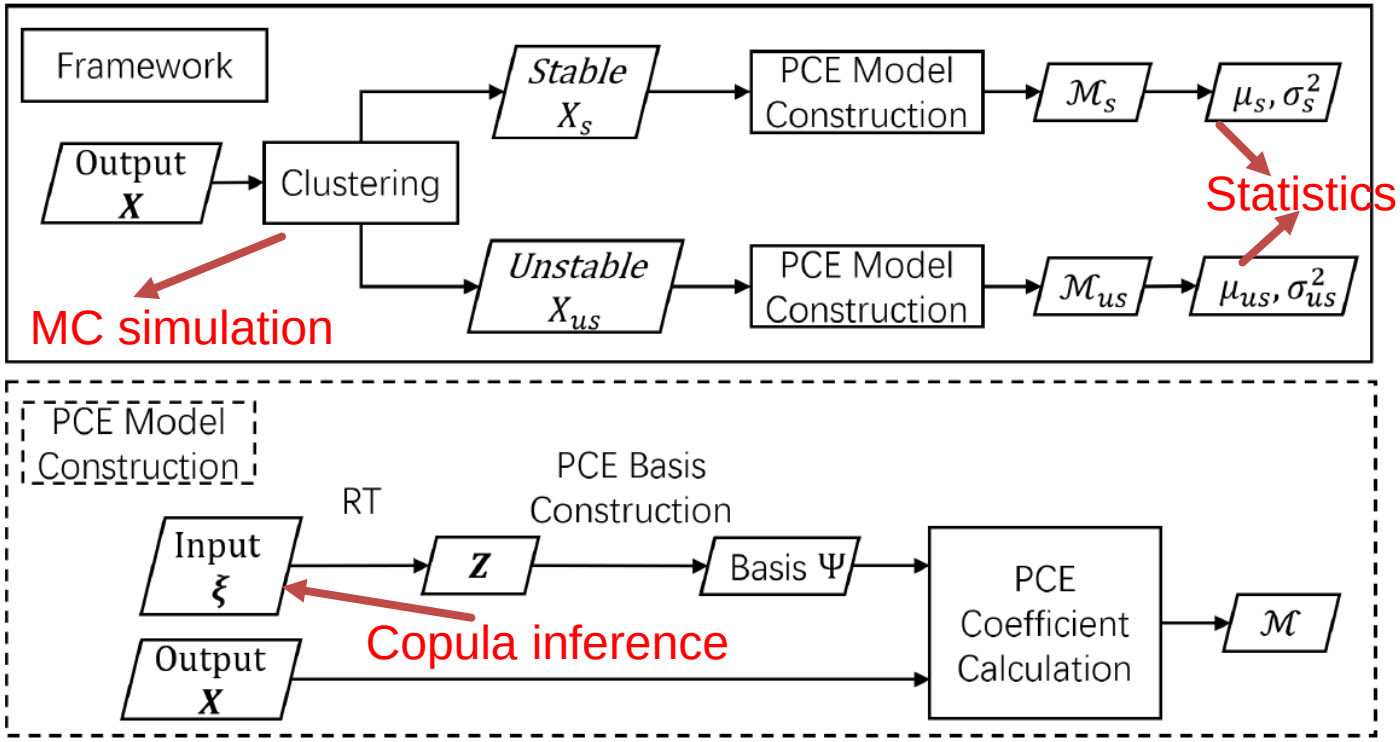

Test Results

- A three-phase fault is applied at bus 16 at 0.5s and is cleared after 10 cycles by opening the line 16-24
- **Uncertain resources**: 3 dynamic loads, 3 dynamic PVs
- **Response**: generator rotor angles
- **Error indicator**: MAPE (Mean absolute percentage error)
- **Comparison approaches**:
  - Latin hypercube sampling
  - PCE
  - CoPCE-PCE considering complicated correlations among loads and IBRs

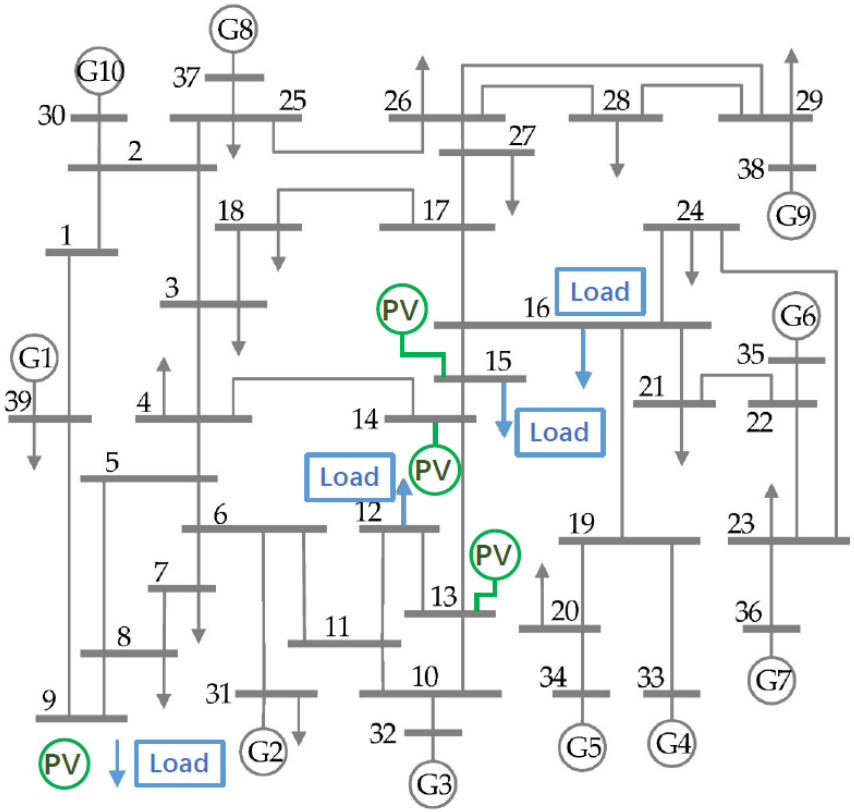

IEEE 39-bus with 10 machines

Results-Nonlinear PV Correlations and Uncertain Loads

NONLINEAR CORRELATIONS OF PVS FOR SCENARIOS 3-5.

Scenarios	Pair Copula type	Parameter
Scenario 3	$[Clayton, Clayton, Clayton]$	$[1.5, 1, 0.5]$
Scenario 4	$[Clayton, Gumbel, Gumbel]$	$[3, 3, 1.2]$
Scenario 5	$[Clayton, Gumbel, Gumbel, Frank, Clayton, Clayton, Gumbel, Gumbel, Frank, Clayton, Clayton, Gumbel, Gumbel, Frank, Clayton]$	$[2, 2, 1.2\ 0.8, 0.5, 2,\ 2, 1.2, 0.8,\ 0.5, 2, 2,\ 1.2, 0.8, 0.5]$

COMPARISON RESULTS OF SCENARIO 3-5

Scenario	Method	Accuracy $e_\mu(\times 10^{-2}\%)$	Accuracy $e_{\sigma^2}(\%)$	CPU time (s)
Scenario 3	MCS	–	–	223.01
	LHS	4.41	2.34	65.48
	PCE	4.24	23.67	15.19
	CoPCE	4.82	1.20	15.56
Scenario 4	MCS	–	–	224.71
	LHS	5.03	2.61	66.20
	PCE	1.21	35.36	15.43
	CoPCE	1.13	0.86	15.70
Scenario 5	MCS	–	–	227.28
	LHS	7.38	2.27	68.52
	PCE	12.50	30.31	28.46
	CoPCE	9.32	1.31	29.11

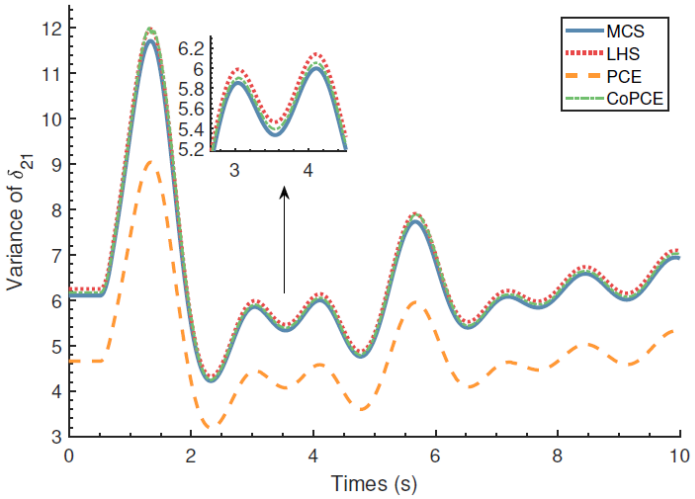

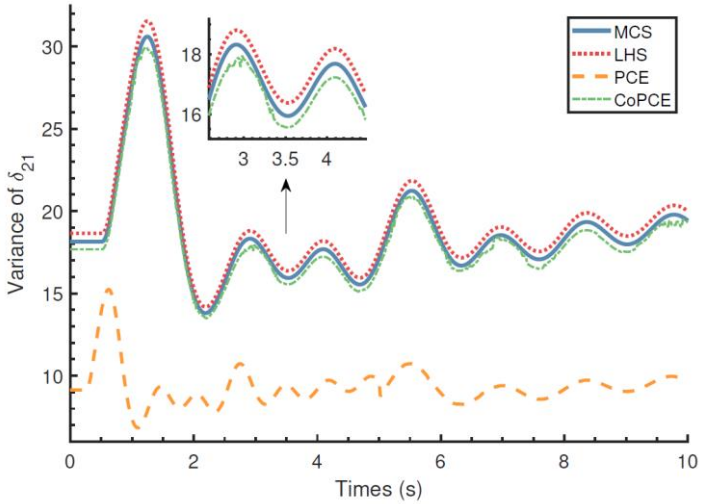

Results-Coexistence of Stable and Unstable Cases

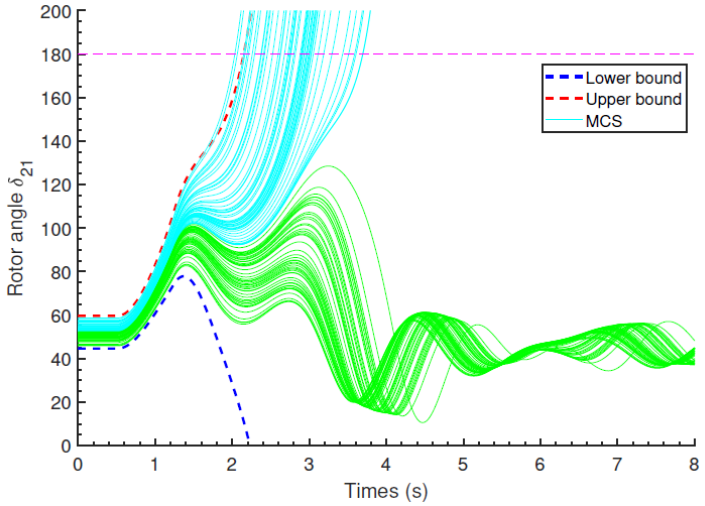

COMPARISON RESULTS OF DIFFERENT METHODS UNDER SCENARIO 6.

Scenario	Method	Accuracy		CPU time (s)
		$e_\mu(\times 10^{-2}\%)$	$e_{\sigma^2}(\%)$	
Scenario 6	MCS	–	–	225.69
	LHS	7.38	2.85	67.93
	PCE	24.98	48.88	28.56
	CoPCE	13.12	2.31	30.08

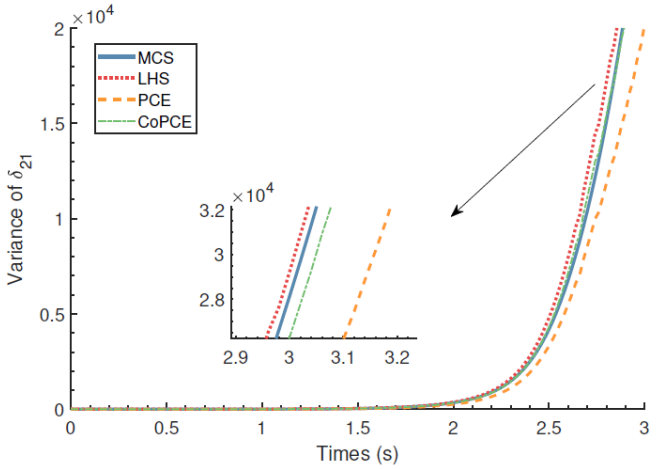

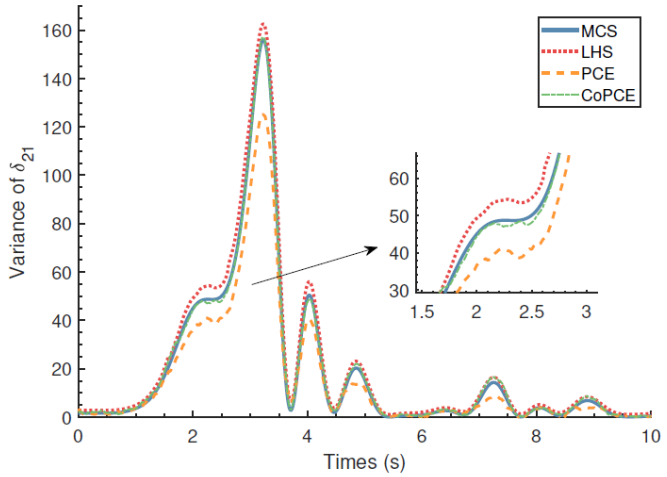

Results-Stochastic Dynamic Security Assessment

Transient stability index

$$TSI = 100 \times \frac{360 - \delta_{max}}{360 + \delta_{max}}$$

δ_{max}: maximum rotor angle deviation

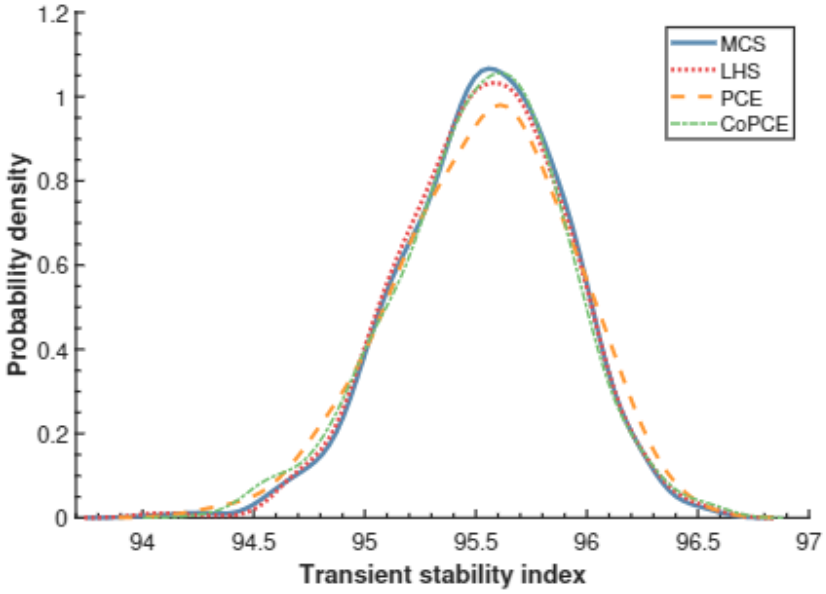

Transient Stable

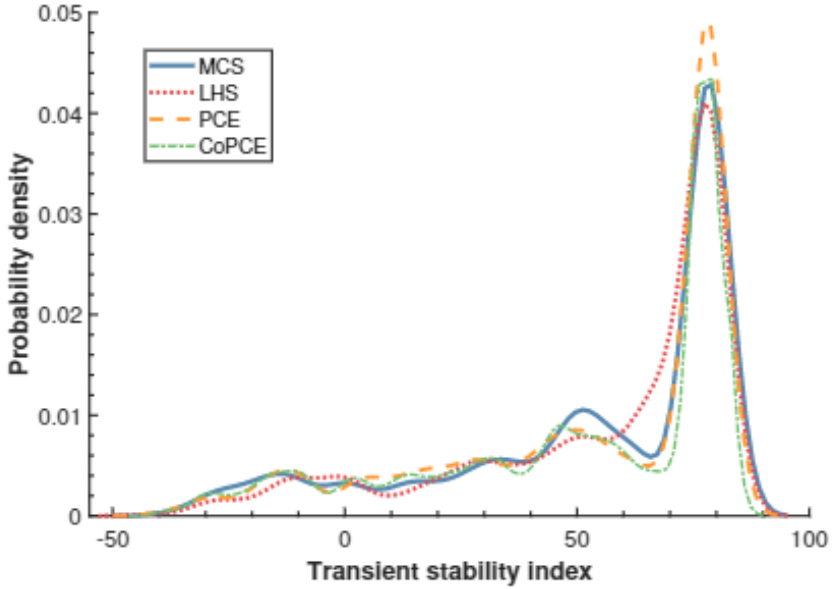

Transient Stable and Unstable

Proposed Method-Scalable to Large-Scale Systems

- **Motivations:**
  - ❖ PCE-based approaches have curse of dimensionality issues when the number of uncertain inputs is large, which is the case for large-scale systems.
  - ❖ PCE-based approaches need to know the probability distribution functions of uncertain inputs, which may be challenging to obtain.
- **Solutions**: develop the **physics-informed sparse Gaussian process-based approach** with high while being scalable to large-scale system.

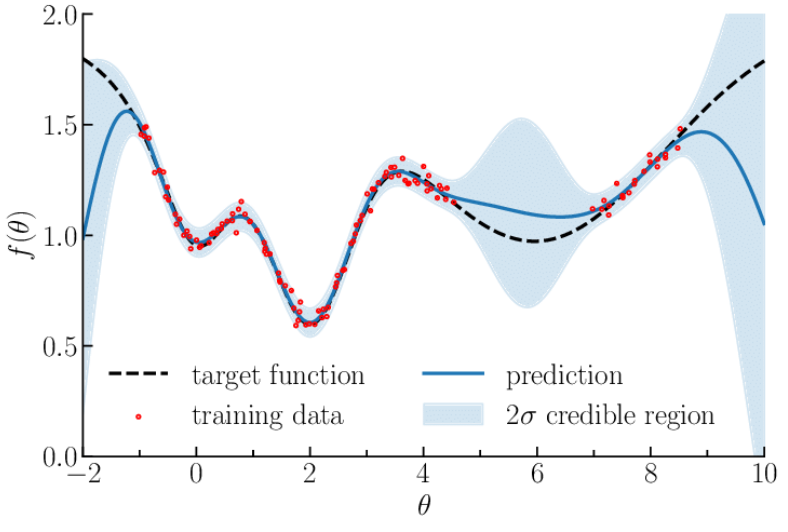

Proposed Method-Scalable to Large-Scale Systems

- **Texas 2000-bus System:**
  - ❖ 100 uncertain dynamic loads and 100 dynamic PVs are designed and placed on the 2000-bus system.
  - ❖ 1000 samples are used for PCE and Gaussian process (GP). Two sets of parameters, 500 samples with 200 inducing points and 400 samples with 100 inducing points (SGP$*$) are tested for sparse GP (SGP).

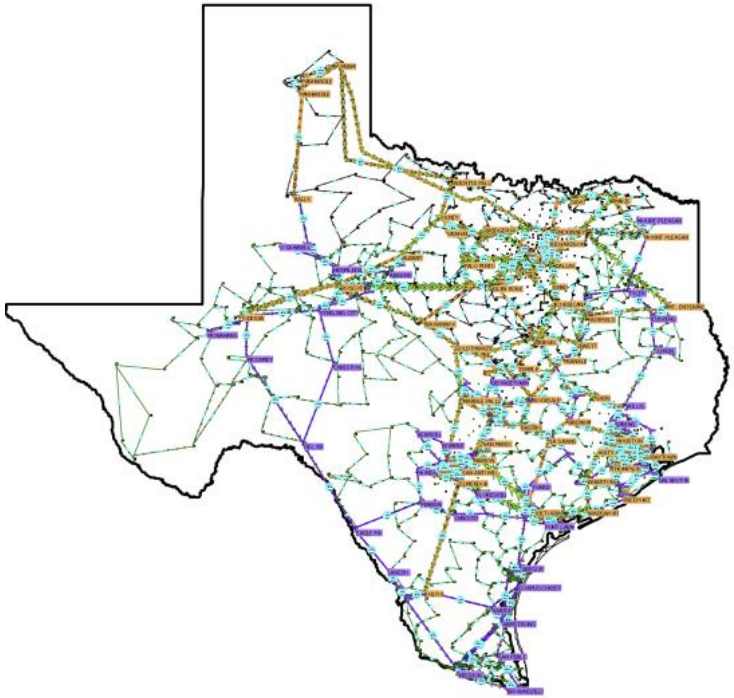

Results on Texas 2000-bus System

- SGP is able to speed up the calculation process while maintaining high accuracy.
- The improvement on accuracy of SGP method over other approaches is significant in terms of stochastic dynamic security assessment.

COMPARISON RESULTS AMONG DIFFERENT METHODS FOR 2000-BUS SYSTEM SCENARIOS 6.

Scenario	Method	Accuracy		CPU time (s)
		$e_\mu(\times 10^{-2}\%)$	$e_{\sigma^2}(\%)$	
Scenario 6 (stable)	MCS	–	–	18637.26
	LHS	5.72	4.40	5931.20
	PCE	19.80	11.41	1805.90
	GP	4.93	5.13	1376.73
	SGP	3.55	3.43	937.45
Scenario 6 (unstable)	MCS	–	–	1876.59
	LHS	10.34	6.59	1927.31
	PCE	13.92	8.86	1823.44
	GP	8.34	4.69	1390.74
	SGP	5.63	3.65	942.24

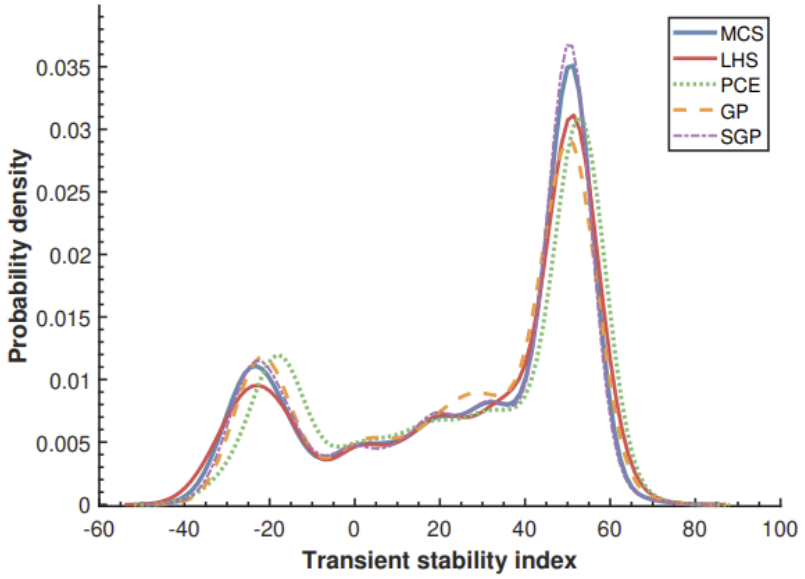

Deep Learning Approach for CMPLDWG Parameter Identification

- As more DERs are integrated into distribution systems, loads' dynamic behavior becomes more difficult to predict.
- WECC has developed the composite load model with distributed generation (CMPLDWG). The proposed model includes static load, different three-phase induction motors, single-phase A/C motors, electronic load, and DERs to accurately describe modern energy grids characteristics.
- Develop a conditional variational autoencoder (CVAE) method for parameter identification to overcome the challenges caused by the nonlinearity of the CMPLDWG model.

Proposed Deep Learning Approach

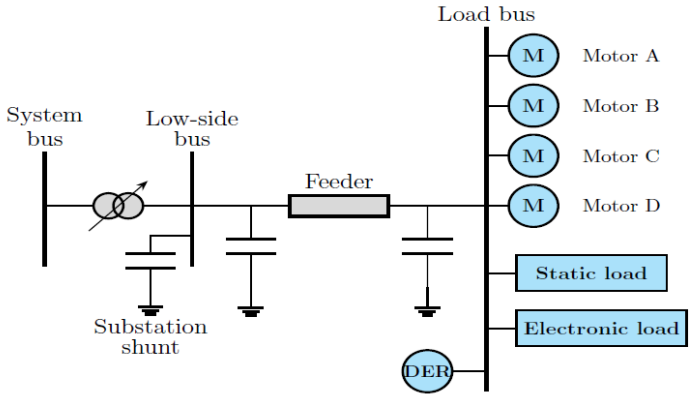

$\boldsymbol{x}$ - CMPLDWG model parameters

$\boldsymbol{y}$ - load bus power and voltage phasor measurements

Offline Training

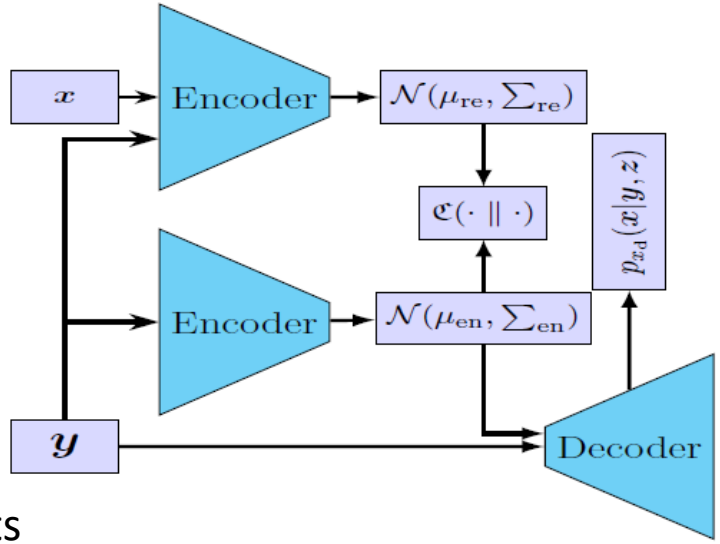

Online Parameter Identification

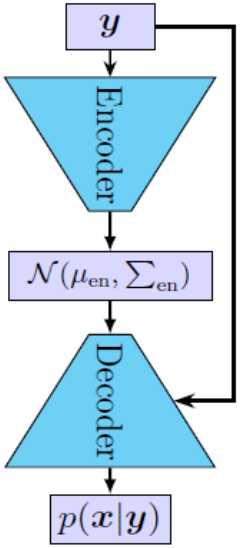

Results

- Event 1: a three-phase fault occurred at bus 6 in the 39-bus system.
- Event 2: a three-phase fault at bus 14 in the 39-bus system.
- Compared with other data-hungry methods that require large sets of disturbances to calibrate, the proposed method only requires a set of reference dynamic responses.

Param.	True Value	Estimated	Param.	True Value	Estimated	Param.	True Value	Estimated	Param.	True Value	Estimated
Motor A			E_{trq}	2	1.95	N_{p2}	3.2	3.22	T_{rf}	0.005	0.005
T_{po}	0.095	0.094	L_a	0.059	0.6	N_{q1}	2	2.1	K_{qv}	1	1
T_{ppo}	0.002	0.002	**Motor C**			N_{q2}	2.5	2.4	T_p	0.025	0.024
L_p	1.8	1.78	T_{po}	0.2	0.21	$CMKPF$	1	0.92	T_{iq}	0.02	0.02
L_{pp}	0.12	0.11	T_{ppo}	0.003	0.003	$CMKQF$	-3.3	-3.32	T_{pord}	0.1	0.1
L_s	0.04	0.41	L_p	1.8	1.82	**Static Load**			K_{pg}	0.1	0.1
R_s	0.104	0.102	L_{pp}	0.19	0.21	P_{1c}	0.648	0.645	K_{ig}	0.05	0.05
H	0.1	0.1	L_s	0.03	0.2	P_{2c}	0.35	0.31	T_g	0.02	0.02
E_{trq}	0.01	0.01	R_s	0.14	0.16	Q_{1c}	1	0.8	T_v	0.2	0.21
L_a	0.059	0.06	H	0.1	0.1	Q_{2c}	0.01	0.01	X_e	0.5	0.5
Motor B			E_{trq}	2	2	P_{freq}	0.001	0.001	L_{fder}	0.75	0.76
T_{po}	0.2	0.18	L_s	0.059	0.06	Q_{freq}	-1	-0.95	**Load Fraction**		
T_{ppo}	0.003	0.003	**Motor D**			**Electronic load**			F_{MA}	0.109	0.10
L_p	1.8	1.75	K_{p1}	0.1	0.1	F_{rcel}	0.6	0.6	F_{MB}	0.114	0.11
L_{pp}	0.19	0.18	K_{p2}	12	11.85	V_{d1}	0.5	0.52	F_{MC}	0.061	0.061
L_s	0.03	0.03	K_{q1}	6	6.1	V_{d2}	0.8	0.76	F_{MD}	0.086	0.85
R_s	0.14	0.135	K_{q2}	11	11.1	**DER A**			F_{el}	0.189	0.19
H	0.5	0.51	N_{p1}	1		T_{rv}	0.008	0.007	P_{fel}	1	1

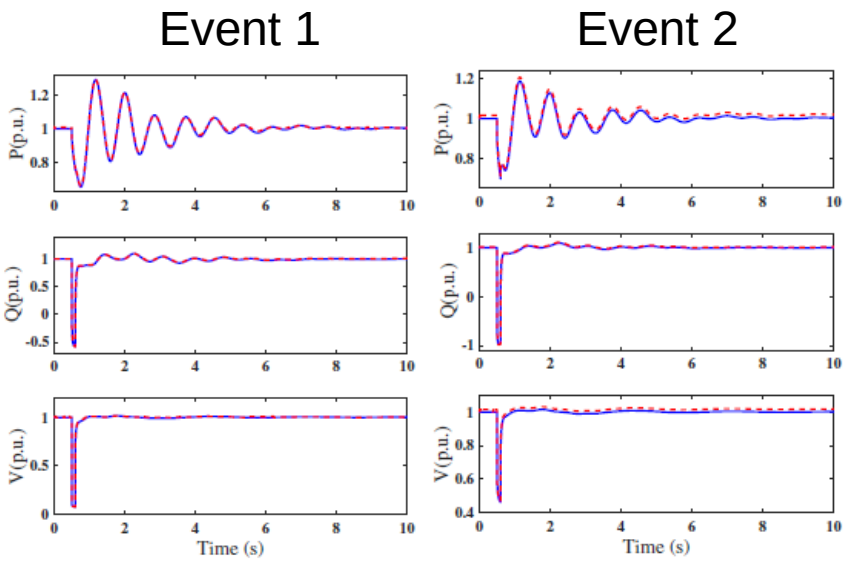

IEEE 2383-bus 327-generator system

- All 1826 loads are represented by 18% Z, 27% I, 45% P, **10%** motor.

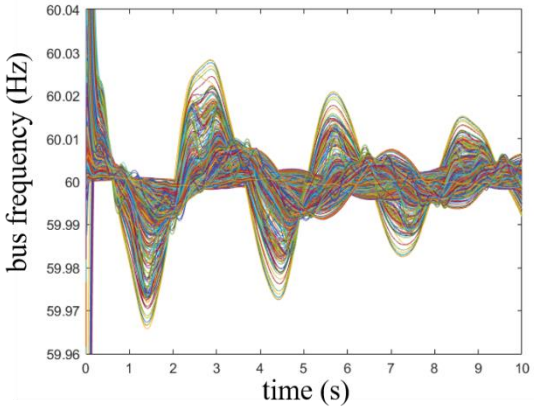

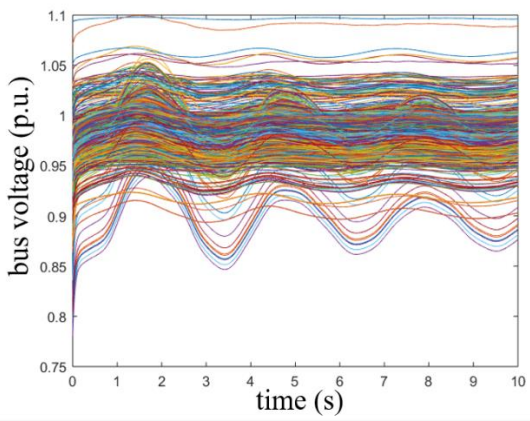

- All 1826 loads are represented by 2% Z, 3% I, 5% P, **90%** motor.

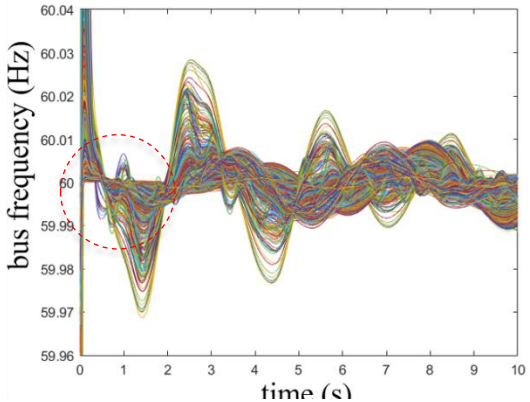

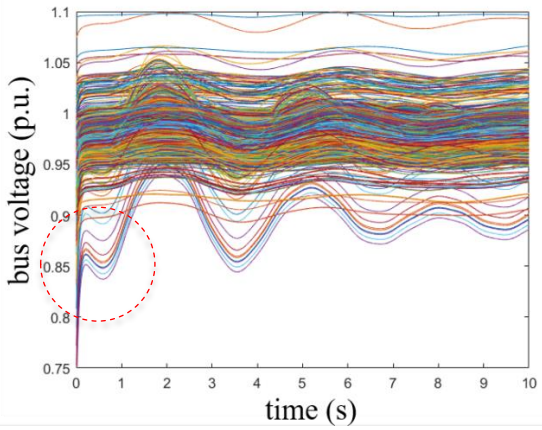

Load Model Reduction

- WECC 179-bus System

  As shown in Fig. 6, only 7 states' nonlinear functions need to be evaluated to represent the dynamic after a 1-cycle 3-phase fault at bus 1.

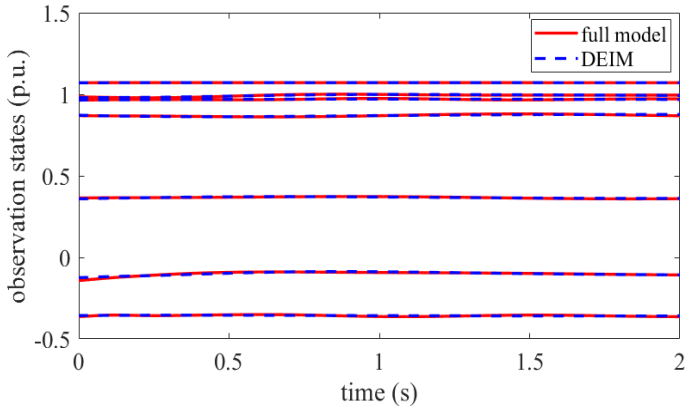

Fig. 6. Observation states comparison of the WECC 179-bus system's full model and DEIM ROM.

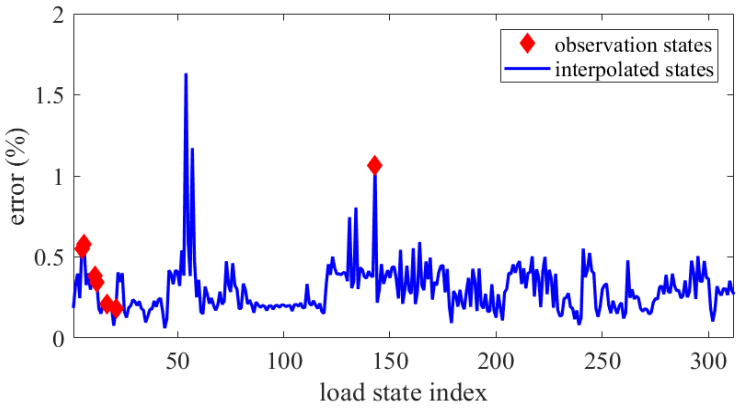

Fig. 7. Normalized error of the WECC 179-bus system load states simulated using DEIM.

Load Model Reduction

A total of 179 simulations with 1-cycle 3-phase bus faults applied to each bus in the system are performed. As shown in Fig. 8, only a small number of load buses have states that are frequently selected by DEIM across all contingencies.

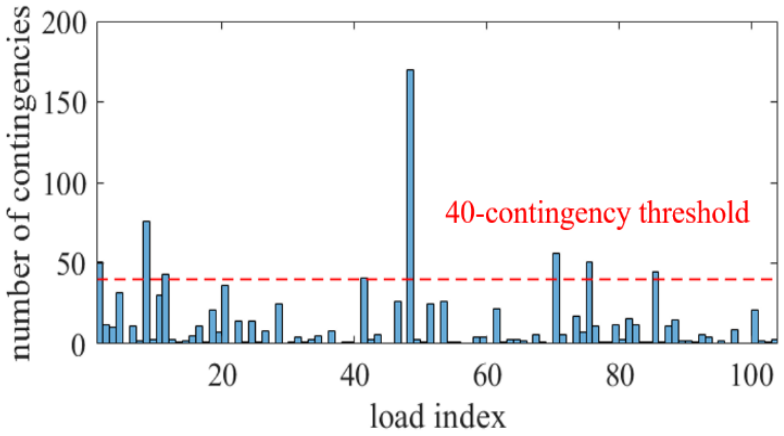

Fig. 8. Number of contingencies for which each load is chosen as observation point in WECC 179-bus system.

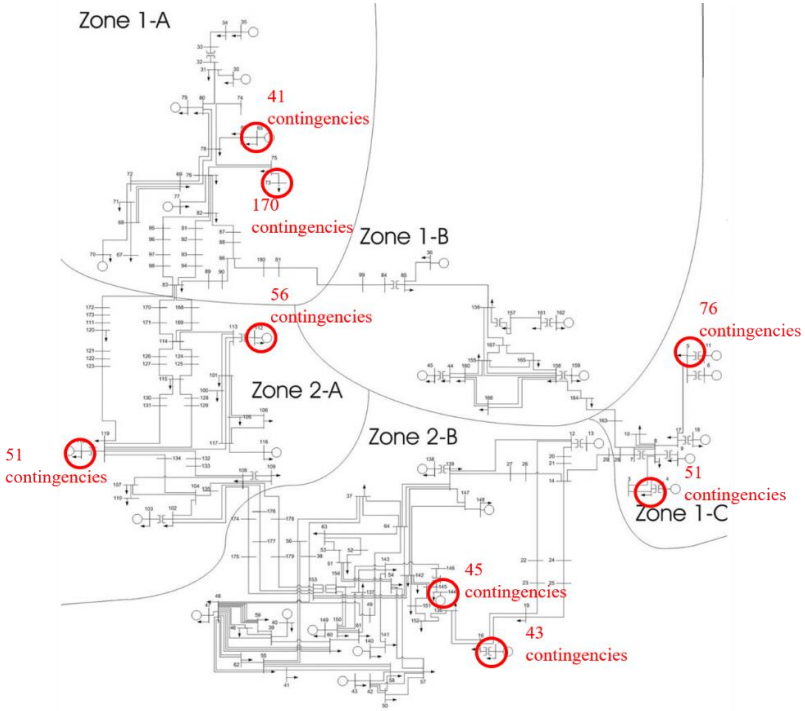

Fig. 9. Locations of load bus most frequently chosen as observation point in WECC 179-bus system.

Summary

Load Sculptor is a tool under development that helps yielding reliable dynamic load models for planning engineers and operators to make important real-time operational decisions for enhancing grid security and stability.

Some capability it currently has are:

- Helping utilities reduce the labor spent on maintaining the accuracy of large load model records;
- Helping the system planners and operators to have significantly enhanced visibility to potential risks caused by variable loads and renewable generations;
- Eliminating the numerical instabilities in the load bus frequency data and makes the data more realistic;
- Prototypical GUI that enables streamlined modification, experimentation, and result visualization

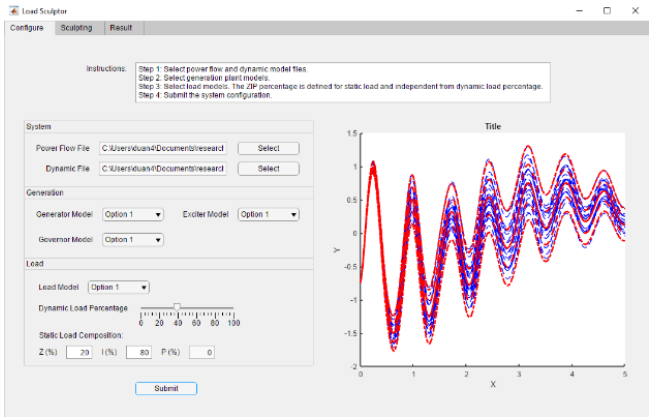

Acknowledgement

This work was supported in part by the U.S. Department of Energy, Office of Electricity, Advanced Grid Modeling Program and in part under the auspices of the U.S. Department of Energy by Lawrence Livermore National Laboratory under Contract DEAC52-07NA27344.

Publications

- K. Ye, J. Zhao, N. Duan. Ye, J. Zhao, N. Duan, D. Maldonado, “Uncertainty Quantification of Loads and Correlated PVs on Power System Dynamic Simulations,” presented at IEEE IAS Industrial & Commercial Power System Asia 2021. (**Best Student Paper Award**)
- N. Duan, J. Zhao, X. Chen, B. Wang, S. Wang, “Discrete empirical interpolation method based dynamic load model reduction,” presented at IEEE PES General Meeting 2021.
- S. R. Khazeiynasab, J. Zhao, N. Duan, “WECC composite load model parameter identification using deep learning approach” to be presented at IEEE PES General Meeting 2022.
- B. Tan, J. Zhao, F. Milano, N. Duan, D. Maldonado, Y. Zhang, H. Zhang, “Distributed Frequency Divider for Power System Bus Frequency Online Estimation Considering Virtual Inertia from DFIGs”, IEEE Journal on Emerging and Selected Topics in Circuits and Systems, vol. 12, no. 1, Mar. 2022.
- K. Ye, J. Zhao, N. Duan, S. Wang, “Quantifying Load and Correlated PV Uncertainties on Power System Dynamic Simulations” submitted to IEEE Transactions on Power Systems.
- K. Ye, J. Zhao, N. Duan, Y. Zhang, H. Zhang, “Data-driven Sparse Gaussian Process for Probabilistic Stability Assessment of Large-Scale Power System with PVs”, submitted to IEEE Transactions on Power Systems.

Backup Slides

Bus Frequency Variation-Background

- The penetration of inverter-based resources (IBRs), such as DFIGs and solar farms, leads to the inertia reduction in the system.
- Control of IBRs as well as dynamic load parameter changes could lead to variations of bus frequency changes.
- Visibility of the bus frequency across the system plays an important role of developing coordinated controls for maintaining low-inertia system stability.

Frequency Monitoring- Challenges

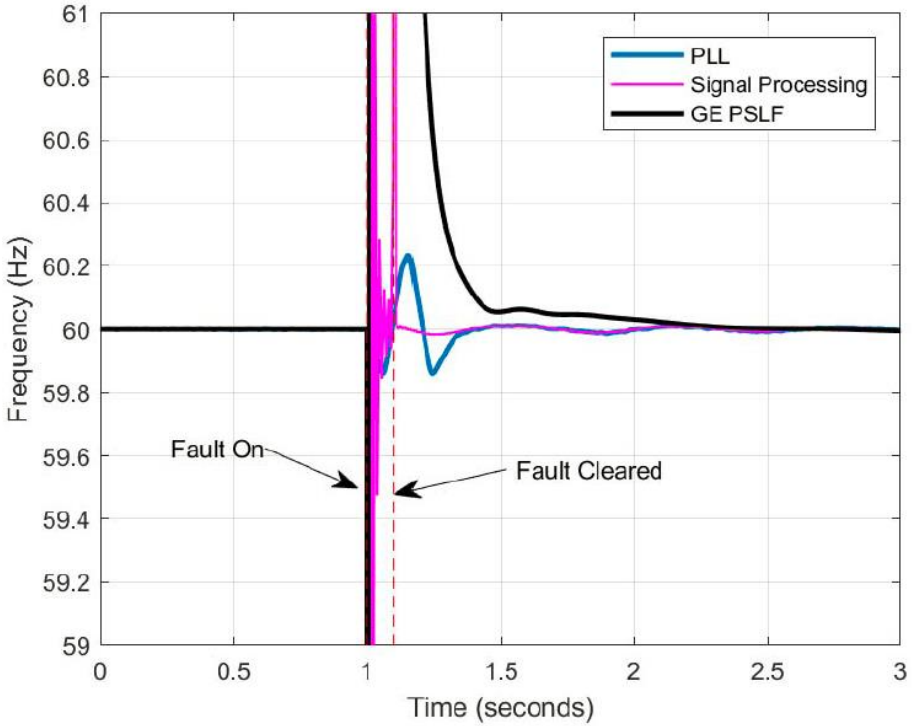

Simulation of a 3-phase fault to ground near a generator

[R3] WECC White Paper on Understanding Frequency Calculation in Positive Sequence Stability Programs

Distributed Frequency Divider Formula (FDF) with DFIGs

- The core idea is to use Thevenin equivalent to approximate the impedance distribution of another area in the power system, and to include the inertia emulation impacts of IBRs, i.e., DFIGs here.

$$diag\left(\boldsymbol{\omega}_B-\omega_0\right)=\tilde{\mathbf{D}}\cdot diag\left(\begin{bmatrix}\boldsymbol{\omega}_G-\omega_0\\ \boldsymbol{\omega}_{VR}-\omega_0\end{bmatrix}\square\begin{bmatrix}\mathbf{1}\\ \boldsymbol{E}_{VR}\end{bmatrix}\right)$$

$$\tilde{\mathbf{D}}=-\left(\mathbf{B}_{BB}+\tilde{\mathbf{B}}_{B0}\right)^{-1}\begin{bmatrix}\mathbf{B}_{BG} & \mathbf{B}_{BR}\end{bmatrix}$$

$$\boldsymbol{\omega}_B=[\omega_{B,1},\ldots,\omega_{B,M-L},\omega_{B,M-L+1},\ldots,\omega_{B,M}]^T$$

$$\boldsymbol{\omega}'_B=[\omega_{B,1},\ldots,\omega_{B,M-L}]^T$$

$$\boldsymbol{\omega}''_B=[\omega_{B,M-L+1},\ldots,\omega_{B,M}]^T$$

Distributed Frequency Divider Formula (FDF)

$$\begin{cases} diag\left((\boldsymbol{\omega}_{VR}-\omega_0)\square\ \boldsymbol{E}_{VR}\right)=\left(\tilde{\mathbf{D}}'''\right)^{-1}*diag\left(\boldsymbol{\omega}''_B-\omega_0\right) \\ \qquad\qquad -\left(\tilde{\mathbf{D}}'''\right)^{-1}\tilde{\mathbf{D}}''\,diag\left(\boldsymbol{\omega}_G-\omega_0\right) \\ diag\left(\boldsymbol{\omega}'_B-\omega_0\right)=\tilde{\mathbf{D}}'\cdot diag\left(\begin{bmatrix}\boldsymbol{\omega}_G-\omega_0\\ \boldsymbol{\omega}_{VR}-\omega_0\end{bmatrix}\square\begin{bmatrix}\mathbf{1}\\ \boldsymbol{E}_{VR}\end{bmatrix}\right) \end{cases}$$

$$\tilde{\mathbf{D}}=\begin{pmatrix}\tilde{\mathbf{D}}'\\ \tilde{\mathbf{D}}''\quad\tilde{\mathbf{D}}'''\end{pmatrix}$$

[R5] B. Tan, J. B. Zhao, et. al, "Distributed Frequency Divider for Power System Bus Frequency Online Estimation Considering Virtual Inertia from DFIGs," IEEE Journal on Emerging and Selected Topics in Circuits and Systems, 2021.

Numerical Results

➢ Simulation Setting

- IEEE 39-bus system is divided into areas A1 and A2.
- The disturbances are all three-phase faults that occur at 1 s and are cleared at 1.1s.
- The frequency estimation results from DIgSILENT PowerFactory and the original FDF are also utilized for comparisons.
- The inertia emulation of DFIG considered in this paper is the droop control based on frequency deviation and ROCOF.

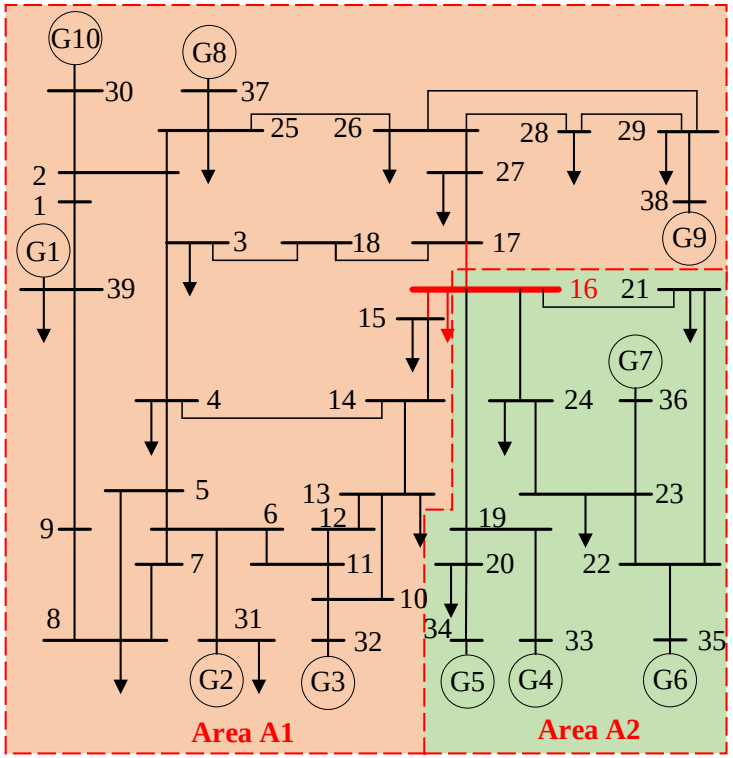

The single-line diagram of the IEEE 39-bus power system

Numerical Results——Distributed FDF without DFIGs

Distributed FDF significantly reduces the frequency estimation errors because the attenuation effect of frequency propagation in the network is included by using boundary true frequency

$$Error = \int_{t_{dis}}^{T} \left| \text{limit}(\boldsymbol{f}_{true}) - \text{limit}(\boldsymbol{f}_{est}) \right| dt \qquad y = \text{limit}(x) = \begin{cases} S_{\max} & if \quad x > S_{\max} \\ S_{\min} & if \quad x < S_{\min} \\ x & Others \end{cases}$$

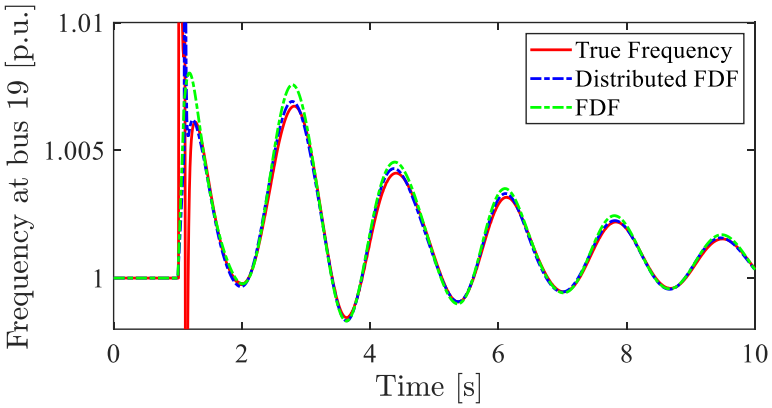

Frequency estimation results for bus 19 by various methods

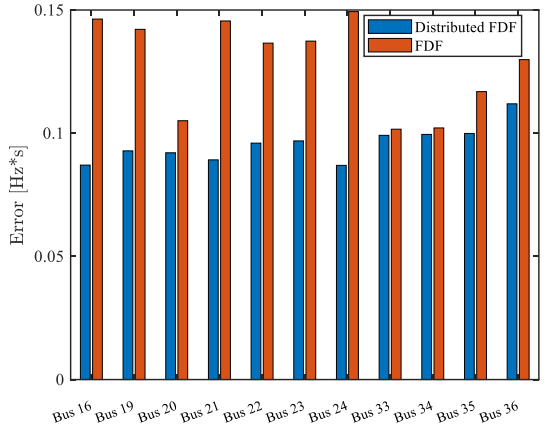

Bus frequency estimation errors comparison

Numerical Results——Distributed FDF with DFIGs

To assess the impacts of the inertia emulation on the proposed method, three sets of inertial control parameters for DFIGs are considered:

$$\Delta P = -R_f \Delta f_b - R_d \frac{df_b}{dt}$$

$$R_f = 10 \quad R_d = 10$$
$$R_f = 20 \quad R_d = 20$$
$$R_f = 30 \quad R_d = 30$$

Control parameters of inertia emulation almost have no impact on the equivalent impedance

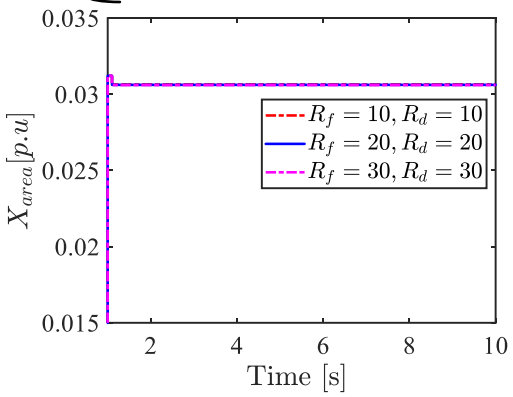

(a)

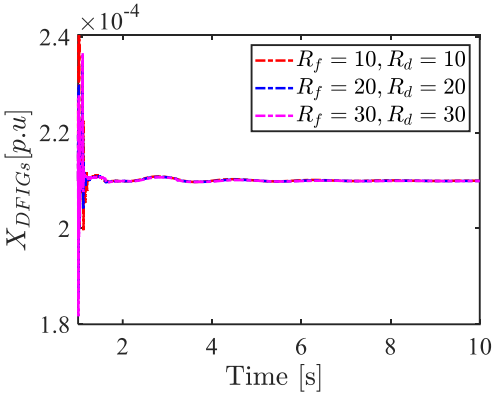

(b)

Equivalent impedance estimation results: (a) for area A1;(b) for DFIGs at bus 36.

Numerical Results—Distributed FDF with DFIGs

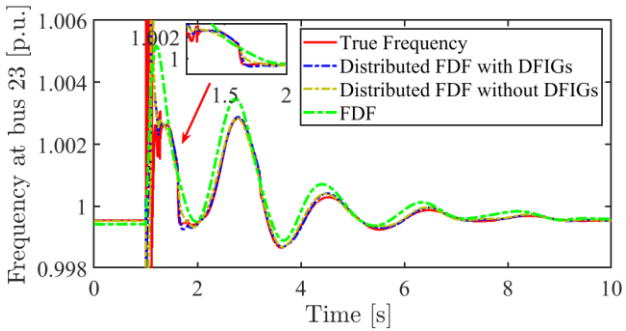

Frequency estimation results for bus 23.

- The stronger the frequency support of DFIGs is, the larger the estimation errors are caused by FDF.
- Distributed FDF with DFIGs can further improve bus frequency estimation accuracy.

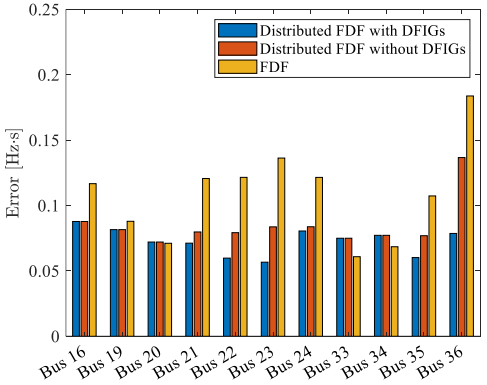

$R_f = 10 \quad R_d = 10$

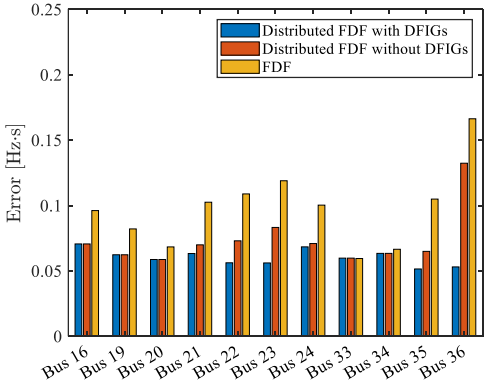

$R_f = 20 \quad R_d = 20$

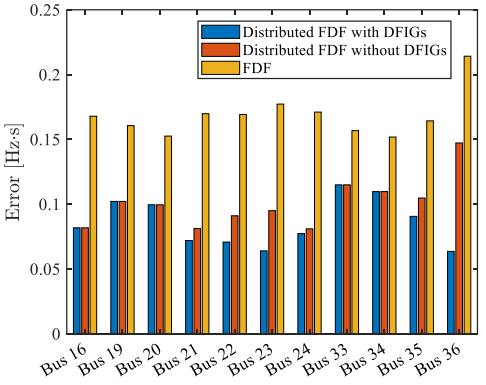

$R_f = 30 \quad R_d = 30$